

Scaling and memory of intraday volatility return intervals in stock markets

Fengzhong Wang,¹ Kazuko Yamasaki,^{1,2} Shlomo Havlin,^{1,3} and H. Eugene Stanley¹

¹Center for Polymer Studies and Department of Physics, Boston University, Boston, MA 02215, USA

²Department of Environmental Sciences, Tokyo University of Information Sciences, Chiba 265-8501, Japan

³Minerva Center and Department of Physics, Bar-Ilan University, Ramat-Gan 52900, Israel

(Received 9 November 2005; published 16 February 2006)

We study the return interval τ between price volatilities that are above a certain threshold q for 31 intraday data sets, including the Standard and Poor's 500 index and the 30 stocks that form the Dow Jones Industrial index. For different threshold q , the probability density function $P_q(\tau)$ scales with the mean interval $\bar{\tau}$ as $P_q(\tau) = \bar{\tau}^{-1} f(\tau/\bar{\tau})$, similar to that found in daily volatilities. Since the intraday records have significantly more data points compared to the daily records, we could probe for much higher thresholds q and still obtain good statistics. We find that the scaling function $f(x)$ is consistent for all 31 intraday data sets in various time resolutions, and the function is well-approximated by the stretched exponential, $f(x) \sim e^{-ax^\gamma}$, with $\gamma = 0.38 \pm 0.05$ and $a = 3.9 \pm 0.5$, which indicates the existence of correlations. We analyze the conditional probability distribution $P_q(\tau|\tau_0)$ for τ following a certain interval τ_0 , and find $P_q(\tau|\tau_0)$ depends on τ_0 , which demonstrates memory in intraday return intervals. Also, we find that the mean conditional interval $\langle \tau|\tau_0 \rangle$ increases with τ_0 , consistent with the memory found for $P_q(\tau|\tau_0)$. Moreover, we find that return interval records, in addition to having short-term correlations as demonstrated by $P_q(\tau|\tau_0)$, have long-term correlations with correlation exponents similar to that of volatility records.

DOI: [10.1103/PhysRevE.73.026117](https://doi.org/10.1103/PhysRevE.73.026117)

PACS number(s): 89.65.Gh, 05.45.Tp, 89.75.Da

I. INTRODUCTION

Statistical properties of price fluctuations [1–15] are very important to understand and model financial market dynamics, which has long been a focus of economic research. Stock volatility is of interest to traders because it quantifies risk, optimizes the portfolio [4,16,17], and provides a key input of option pricing models that are based on the estimation of the volatility of the asset [17–20]. Although the logarithmic changes of stock price from time $t-1$ to time t ,

$$G(t) \equiv \log\left(\frac{p_t}{p_{t-1}}\right), \quad (1)$$

are only short-term correlated, their absolute values are known to be long-term power-law correlated [21–33]. The probability density function (PDF) of $|G(t)|$ possesses a power-law tail,

$$\Phi(|G|) \sim |G|^{-(\zeta+1)}, \quad (2)$$

with $\zeta \approx 3$, and the PDF of $G(t)$ also has a power-law tail with the same value of the exponent ζ [3,33–38]

$$\Phi(G) \sim G^{-(\zeta+1)}. \quad (3)$$

A possible explanation of Eq. (3) involves the distribution obtained by convolving many different Gaussians, with log-normally distributed variance [39,40]. Also, $n_q(t)$, the number of times that the volatility $|G(t)|$ exceeds a threshold q , follows a power law in the time t after a market crash,

$$n_q(t) \sim t^{-p}, \quad (4)$$

with $p \approx 1$ [41]. Equation (4) is the financial analog of the Omori earthquake law [42].

Recently Yamasaki *et al.* [43] studied the behavior of return intervals τ between volatilities that are above a certain

threshold q [illustrated in Fig. 1(a)]. They analyzed *daily* financial records and found scaling and memory in return intervals, similar to that found in climate data [44]. To investigate the generality of these statistical features of Ref. [43], here we examine 31 *intraday* data sets. We find that similar scaling and memory behavior occurs at a wide range of time resolutions (not only on the daily scale). Due to the larger size of the data sets we analyze, we are able to extend our work to significantly larger values of q . Remarkably, scaling functions are well-approximated by the stretched exponential form, which indicates long-range correlations in volatility records [44]. Also, we explore clusters of short and long return intervals, and find that the larger the cluster is the stronger is the memory.

II. DATABASES ANALYZED

We analyze the trades and quotes (TAQ) database from the New York Stock Exchange (NYSE), which records every trade for all the securities in the United States stock market for the 2-year period from January 1, 2001 to December 31, 2002, a total of 497 trading days. We study all 30 companies of the Dow Jones Industrial Average index (DJIA). The sampling time is 1 min and the average size is about 160,000 values per DJIA stock. Another database we analyze is the Standard and Poor's 500 index (S&P 500), which consists of 500 companies. This database is for a 13-year period, from January 1, 1984 to December 31, 1996, with one data point every 10 min (total data points is about 130,000). For both databases, the records are continuous in regular open hours for all trading days, due to the removal of all market closure times.

III. VOLATILITY DEFINITION

In contrast to daily volatilities, the intraday data are known to show specific patterns [23,24,33], due to different

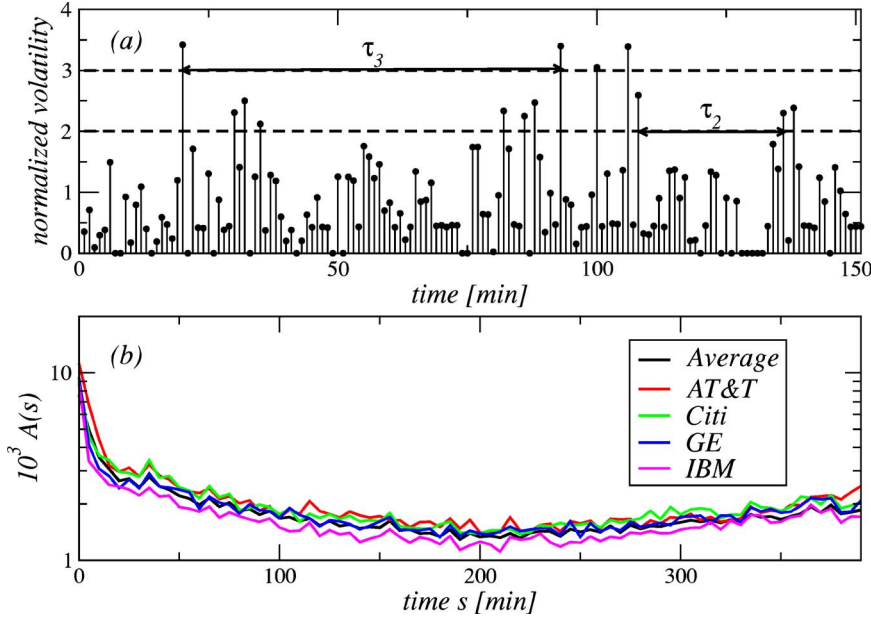


FIG. 1. (Color online) (a) Illustration of volatility return intervals for a volatility time series for IBM on May 10, 2002. Return intervals τ_3 and τ_2 for two thresholds $q=3$ and 2 are displayed. (b) The 5-min interval intraday pattern for AT&T, Citi, GE, IBM, and the average over 30 DJIA stocks. The time s is the moment in each day, while $A(s)$ is the mean return over all trading days. Note that all curves have a similar pattern, such as a pronounced peak after the market opens and a minimum around noon ($s \approx 200$ min).

behaviors of traders at different periods during the trading day. For example, the market is very active immediately after the opening [24] due to information arriving while the market is closed. To understand the possible effect on volatility correlations, we investigate the daily trend in DJIA stocks. The intraday pattern, denoted as $A(s)$ [33], is defined as

$$A(s) \equiv \frac{\sum_{i=1}^N |G^i(s)|}{N}, \quad (5)$$

which is the return at a specific moment s of the day averaged over all N trading days, and $G^i(s)$ is the price change at time s in day i . As shown in Fig. 1(b), the intraday pattern $A(s)$ has similar behavior for the four stocks AT&T, Citi, GE, and IBM and the average over 30 DJIA stocks. The pattern is not uniformly distributed, exhibiting a pronounced peak at the opening hours and a minimum around time $s=200$ min that may cause some artificial correlations. To avoid the effect of this daily oscillation, we remove the intraday pattern by studying

$$G'(t) \equiv |G(t)|/A(s). \quad (6)$$

In order to compare different stocks, we define the normalized volatility $g(t)$ by dividing $G'(t)$ with its standard deviation,

$$g(t) \equiv \frac{G'(t)}{(\langle G'(t)^2 \rangle - \langle G'(t) \rangle^2)^{1/2}}, \quad (7)$$

where $\langle \dots \rangle$ is the time average for each separate stock. Consequently, the threshold q is measured in units of the standard deviation of $G'(t)$. As shown in Fig. 1(a), every volatility $g(t)$ above a threshold q (“event”) is picked and the series of the time intervals between those events, $\{\tau(q)\}$, is generated. The series depends on the threshold q . To maintain good statistics and avoid spurious discreteness effects [43], we restrict ourselves to thresholds with average inter-

vals $\bar{\tau} = \bar{\tau}(q) > 3$ time units (30 min for the S&P 500 and 3 min for the 30 stocks of the DJIA).

IV. SCALING PROPERTIES

We study the dependence of $P_q(\tau)$ on q , where $P_q(\tau)$ is the PDF of the return interval series $\{\tau(q)\}$. Figure 2 shows results for the S&P 500 index and for two typical DJIA stocks, Citi and GE. The time window Δt of volatility records is 1 min for the DJIA stocks and 10 min for the S&P 500. The left panels of Fig. 2 [(a), (c), and (e)] show that the PDF $P_q(\tau)$ for large q decays slower than for small q . The right panels of Fig. 2 [(b), (d), and (f)] show the *scaled* PDF $P_q(\tau)\bar{\tau}$ as a function of the *scaled* return intervals $\tau/\bar{\tau}$. The five curves for $q=2, 3, 4, 5$, and 6 collapse onto a single curve. Thus the distribution functions follow the scaling relation [43,45]

$$P_q(\tau) = \frac{1}{\bar{\tau}} f(\tau/\bar{\tau}). \quad (8)$$

We also study the other 28 DJIA stocks and find that they have similar scaling behavior for different thresholds.

To examine the scaling for larger thresholds with good statistics, we calculate the return intervals of each DJIA stock, and then aggregate all the data. As shown in Figs. 2(g) and 2(h), the scaling behavior extends even to $q=15$. In Eq. (8), the scaling function $f(\tau/\bar{\tau})$ does not directly depend on the threshold q but only through $\bar{\tau} \equiv \bar{\tau}(q)$. Therefore if $P_q(\tau)$ for an individual value of q is known, distributions for other thresholds can be predicted by the scaling Eq. (8). In particular, the distribution of rare events (very large q , such as market crashes) may be extrapolated from smaller thresholds, which have enough data to achieve good statistics.

Next, we investigate the similarity of scaling functions for different companies. Scaled PDFs $P_q(\tau)\bar{\tau}$ with $q=2$ for return intervals (upper symbols) are plotted in Fig. 3(a), showing the S&P 500 index and 30 DJIA stocks in alphabetical

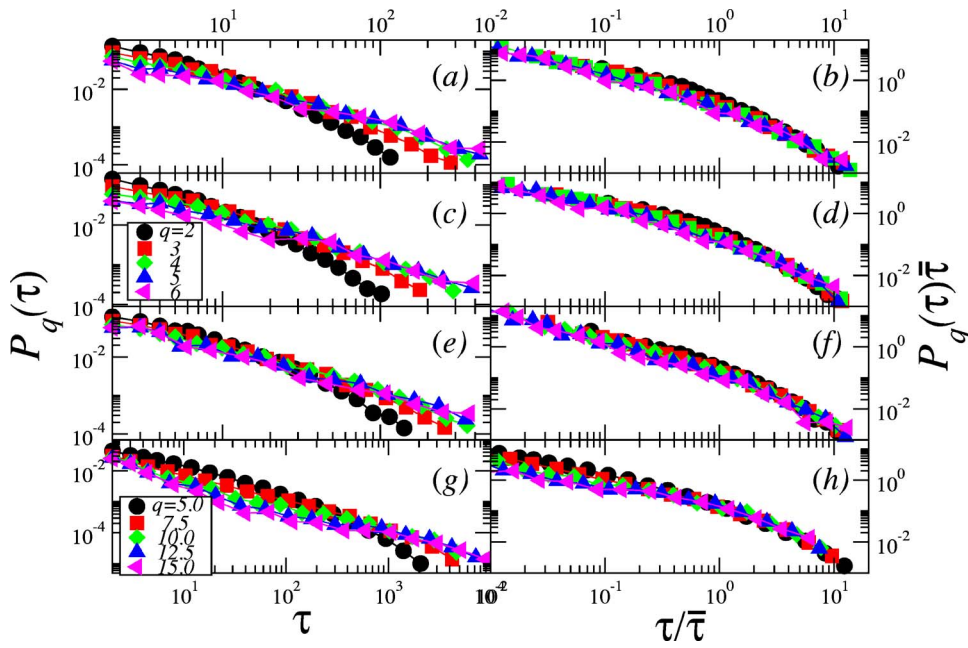


FIG. 2. (Color online) Distribution and scaling of return intervals for (a) and (b) Citi, (c) and (d) GE, (e) and (f) S&P 500, and (g) and (h) mixture of 30 DJIA stocks (for very large thresholds). Symbols are for different threshold q , as shown in (c) for (a)–(f) and shown in (g) for (g) and (h). The sampling time for S&P 500 is 10 min, and for the stocks is 1 min. For one dataset, the distributions $P_q(\tau)$ are different with different q , but they collapse onto a single curve for $P_q(\tau)\bar{\tau}$ vs $\tau/\bar{\tau}$ ($\bar{\tau}$ is the mean interval), which indicates a scaling relation. (g) and (h) show that the scaling can extend to very large thresholds.

order of names (one symbol represents one dataset). We see that the PDF curves collapse, so their scaling functions $f(x)$ are similar, consistent with a universal structure for $P_q(\tau)$. As suggested by the line on upper symbols in Fig. 3(a) and on the closed symbols in Fig. 4, the function $f(x)$ may follow a stretched exponential form [44],

$$f(x) \sim e^{-ax^\gamma}. \tag{9}$$

Remarkably, we find that all 31 datasets have similar exponent values, and conclude that γ appears to be “universal,” with

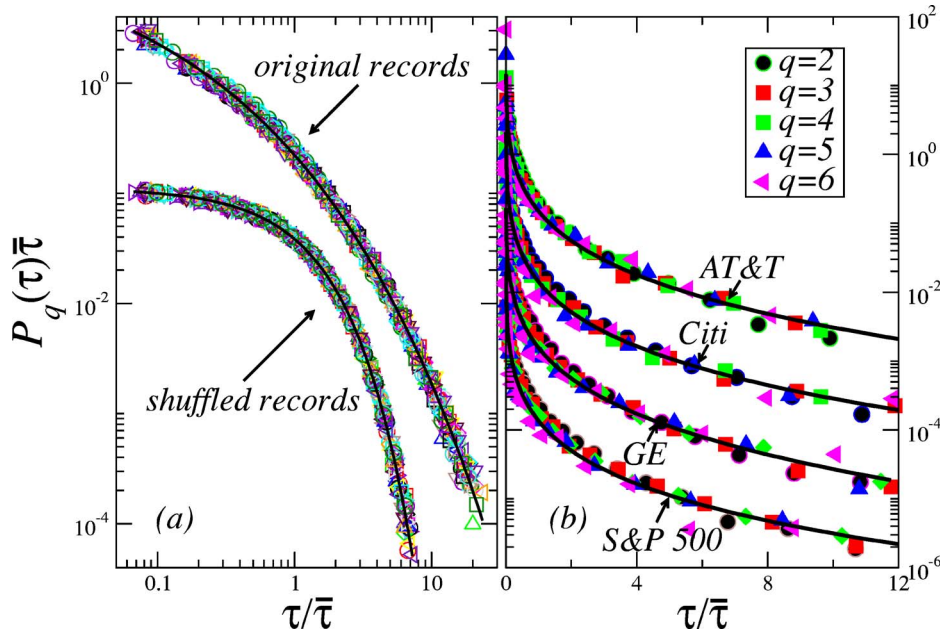


FIG. 3. (Color online) (a) Scaling of return intervals for all 30 DJIA stocks and S&P 500 index. Scaled distribution function $P_q(\tau)\bar{\tau}$ vs $\tau/\bar{\tau}$ with threshold $q=2$ for actual return intervals, as well as for the shuffled volatility records (divided by 10), are shown. Every symbol represents one stock. The line on the symbols for original records suggests a stretched exponential relation, $f(x) \sim e^{-ax^\gamma}$ with $\gamma \approx 0.38 \pm 0.05$ and $a \approx 3.9 \pm 0.5$, while the curve fitting the shuffled records is exponential, $y = e^{-bx}$, from a Poisson distribution. Note that all the datasets are consistent with a single scaling relation. A Poisson distribution indicates no correlation in shuffled volatility data, but the stretched exponential behavior indicates strong correlation in the volatilities (see [44]). (b) Stretched exponential fit for AT&T, Citi, GE, and S&P 500 all with $\gamma=0.4$. Each stock is well-approximated by stretched exponential for diverse thresholds, $q=2, 3, 4, 5$, and 6 , presented in the plot. Each plot is shifted by $\times 10$ for clarity.

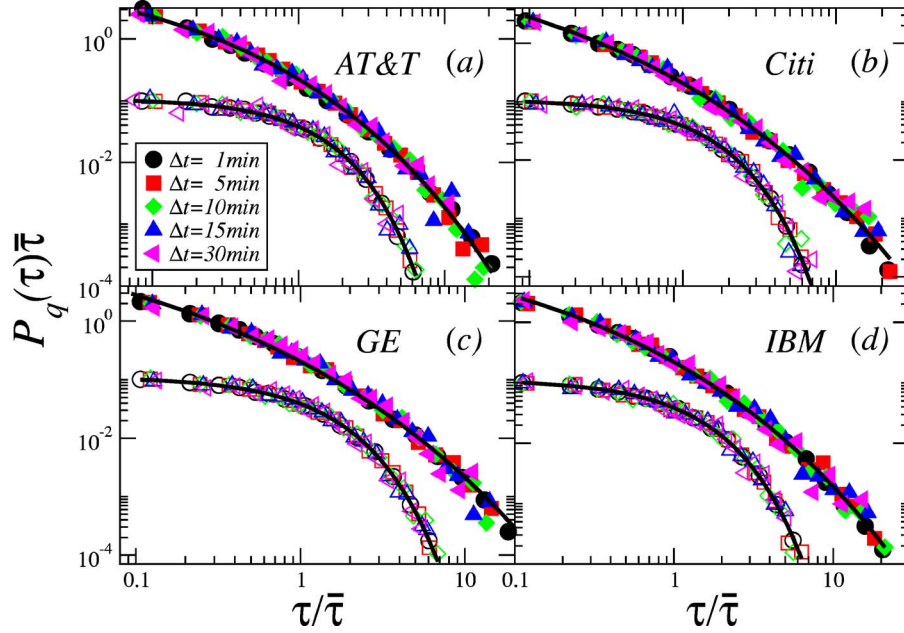


FIG. 4. (Color online) Scaling for different time windows, $\Delta t=1, 5, 10, 15,$ and 30 min. Plots display scaled PDF $P_q(\tau)\bar{\tau}$ with threshold $q=2$ for volatility return intervals (closed symbols) and shuffled volatility records (shifted by factor 10, open symbols) vs $\tau/\bar{\tau}$ of (a) AT&T, (b) Citi, (c) GE, and (d) IBM. Each symbol represents one scale Δt , as shown in (a). Similar to Figs. 2 and 3, curves fall onto a single line for actual return intervals and shuffled data, respectively, which indicates the scaling relation in Eq. (9). Also, the actual return intervals suggest a stretched exponential scaling function, demonstrated by the line fitting the solid symbols. The stretched exponential is a result of the long-term correlations in the volatility records. The shuffled volatility records display no correlation, indicated by the good fit (solid line) to the Poisson distribution.

$$\gamma = 0.38 \pm 0.05. \quad (10)$$

The value a is found to be almost the same for all data sets,

$$a = 3.9 \pm 0.5. \quad (11)$$

Further, we plot the stretched exponential fit for four companies, AT&T, Citi, GE, and IBM in a log-linear plot [Fig. 3(b)]. We find good fits for all four companies, and we also find good collapse for different thresholds for each stock. The scaling function clearly differs from the Poisson distribution for uncorrelated data, $f(x) \sim e^{-x}$, which is demonstrated by curves on lower symbols in Fig. 3(a).

For statistical systems, the time resolution of records is an important aspect. The system may exhibit diverse behavior in different time windows Δt . In Fig. 4 we analyze five time scales for four typical companies ($q=2$): (a) AT&T, (b) Citi, (c) GE, and (d) IBM. It is seen that for $\Delta t=1, 5, 10, 15,$ and 30 min, the $P_q(\tau)\bar{\tau}$ curves collapse onto one curve, which shows the persistence of the scaling for a broad range of time scales. Thus there seems to be a universal structure for stocks not only in different companies, but also in each stock with various time resolutions. For a related study of persistence in different time scales of financial markets, see [46].

To understand the origin of the scaling behavior in return intervals, we analyze PDFs of the volatility after shuffling (in order to remove correlations in the volatility records [33,43]). For uncorrelated data, as expected, a Poisson distribution is obtained, shown by the lower symbols in Fig. 3(a) and open symbols in Fig. 4. In contrast to the distribution for uncorrelated records, the distribution of the actual

return intervals [the upper symbols in Fig. 3(a) and closed symbols in Fig. 4] is more frequent for both small and large intervals, and less frequent in intermediate intervals. The distinct difference between the distributions of return intervals in the original data and shuffled records suggests that the scaling behavior and the form in Eq. (9) must arise from long-term correlations in the volatility (see also [44]).

V. MEMORY EFFECTS

The sequence of return intervals may, or may not, be fully characterized by $P_q(\tau)$, depending on the time organization of the sequence. If the sequence of return intervals is *uncorrelated*, the return intervals are independent of each other and totally determined by the probability distribution. On the other hand, if the intervals are *correlated*, the memory will also affect the order in the sequence of intervals.

To investigate the memory in the records, we study the conditional PDF, $P_q(\tau|\tau_0)$, which is the probability of finding a return interval τ immediately after a return interval of size τ_0 . In records without memory, $P_q(\tau|\tau_0)$ should be identical to $P_q(\tau)$ and independent of τ_0 . Otherwise, it should depend on τ_0 . Due to the poor statistics for a single τ_0 , we study $P_q(\tau|\tau_0)$ for a bin (range) of τ_0 . The entire database is partitioned into eight equal-size bins with intervals in increasing length. Figure 5 shows $P_q(\tau|\tau_0)$ for τ_0 in the smallest (closed symbols) and largest (open symbols) subset of the four stocks AT&T, Citi, GE, and IBM. For τ_0 in the lowest bin the probability is larger for small τ , while for τ_0 in the largest bin

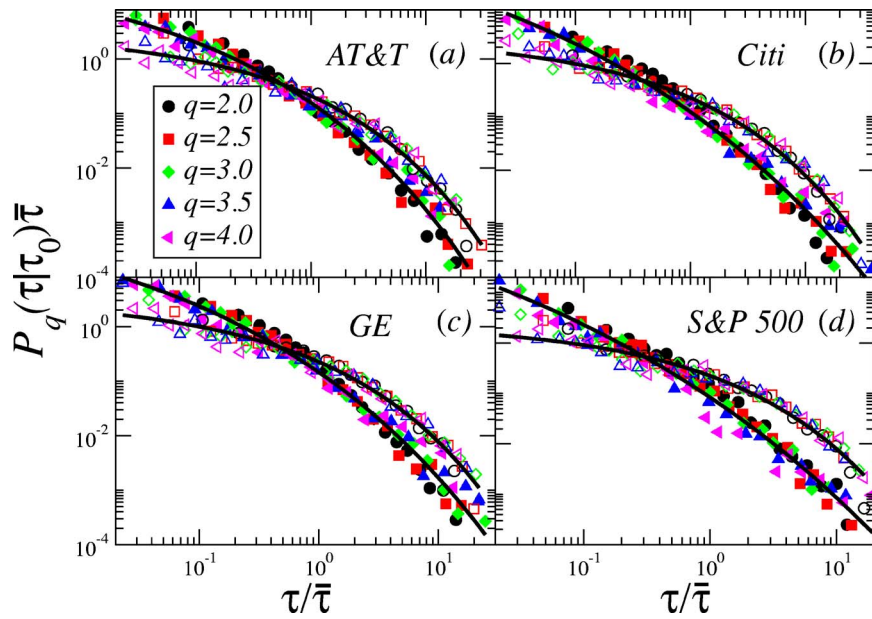


FIG. 5. (Color online) Scaled conditional distribution $P_q(\tau|\tau_0)\bar{\tau}$ vs $\tau/\bar{\tau}$ for (a) AT&T, (b) Citi, (c) GE, and (d) S&P 500. Here τ_0 represents binning of a subset which contains 1/8 of the total number of return intervals in increasing order. Lowest 1/8 subset (closed symbols) and largest 1/8 subset (open symbols) are displayed, which have a different tendency, as suggested by black curves. Symbols are plotted for different thresholds, denoted in (a). In contrast to the largest subset, the lowest bin has larger probability for small intervals and smaller probability for large values, which indicates memory in records: small intervals tend to follow small ones and large intervals tend to follow large ones. Solid curves on symbols are stretched exponential fits.

the probability is higher for large τ . Thus large τ_0 tend to be followed by large τ , while small τ_0 tend to be followed by small τ (“clustering”), which indicates memory in the return interval sequence. Thus long-term correlations in the volatility records affect the PDF of intervals as well as the time organization of τ . Note also that $P_q(\tau|\tau_0)$ for all thresholds seems to collapse onto a single scaling function for each of the τ_0 subsets.

Further, the memory is also seen in the mean conditional return interval $\langle \tau|\tau_0 \rangle$, which is the first moment of $P_q(\tau|\tau_0)$,

immediately after a given τ_0 subset. Closed symbols in Fig. 6 show again that large τ tend to follow large τ_0 , and small τ follow small τ_0 , similar to the clustering in the conditional PDF $P_q(\tau|\tau_0)$. Correspondingly, shuffled data (open symbols) exhibit a flat shape, demonstrating that the value of τ is independent of the previous interval τ_0 .

The quantities $P_q(\tau|\tau_0)$ and $\langle \tau|\tau_0 \rangle$ show memory for intervals that immediately follow an interval τ_0 , which indicates short-term memory in the return interval records. To study the possibility that the long-term memory exists in the

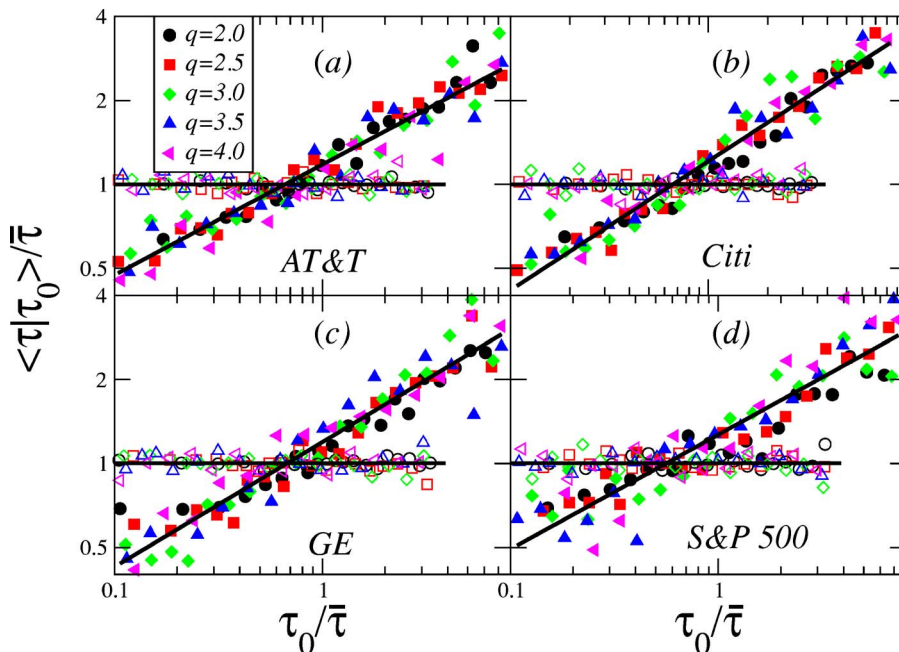


FIG. 6. (Color online) Scaled mean conditional return interval $\langle \tau|\tau_0 \rangle/\bar{\tau}$ vs $\tau_0/\bar{\tau}$ for (a) AT&T, (b) Citi, (c) GE, and (d) S&P 500. The $\langle \tau|\tau_0 \rangle/\bar{\tau}$ of intervals (closed symbols) and shuffled records (open symbols) are plotted. Five thresholds, $q=2.0, 2.5, 3.0, 3.5,$ and 4.0 are represented by different symbols, as shown in (a). The distinct difference between actual intervals and shuffled records implies memory in the original interval records.

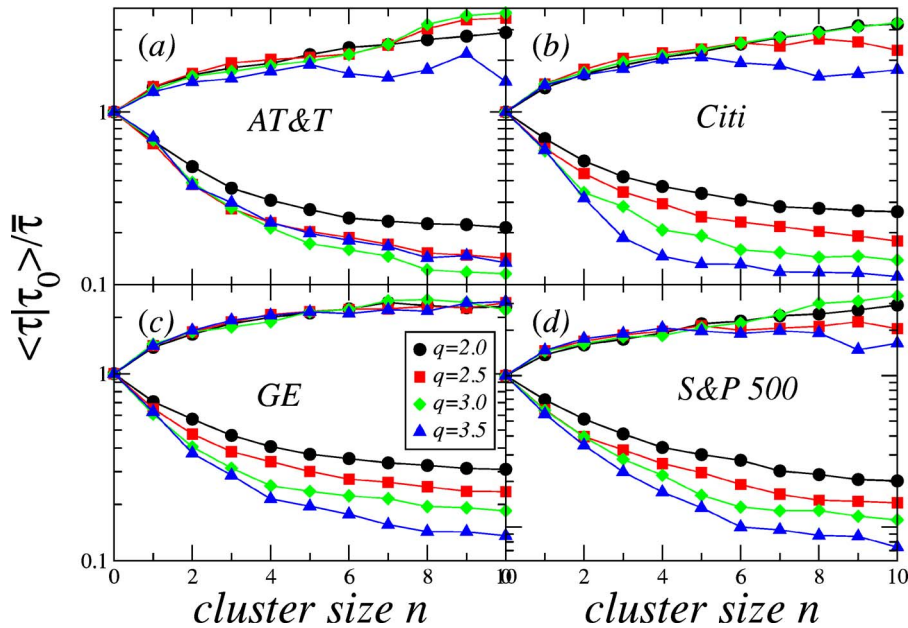


FIG. 7. (Color online) Memory in return interval clusters. τ_0 represents a cluster of intervals, consisting of n consecutive values that all are above (denoted as “+”) or below (“-”) the median of the entire interval records. Plots display the scaled mean interval conditioned on a cluster, $\langle \tau | \tau_0 \rangle / \bar{\tau}$ vs the size n of the cluster for (a) AT&T, (b) Citi, (c) GE, and (d) S&P 500. One symbol shows one threshold q , as shown in (c). The upper part of curves is for “+” clusters while the lower part is for “-” clusters. The plots show that “+” clusters are likely to be followed by large intervals, and “-” clusters by small intervals, consistent with long-term memory in return interval records.

return intervals sequence, we investigate the mean return interval after a cluster of n intervals, all within a bin τ_0 . To obtain good statistics we divide the sequence only into two bins, separated by the median of the entire database. We denote intervals that are above the median by “+” and that are below the median by “-.” Accordingly, n consecutive “+” or “-” intervals form a cluster and the mean of the return intervals after such n -clusters may reveal the range of memory in the sequence. Figure 7 shows the mean return intervals $\langle \tau | \tau_0 \rangle / \bar{\tau}$ vs the size n , where τ_0 in $\langle \tau | \tau_0 \rangle / \bar{\tau}$ refers to a cluster with size n . For “+” clusters, the mean intervals increase with the size of the cluster, the opposite of that for “-” clusters. The results indicate long-term memory in the sequence of τ since we do not see a plateau for large clusters.

To further test the range of long-term correlations in the return interval time series, we apply the detrended fluctuation analysis (DFA) method [47–49]. After removing trends, the DFA method computes the root-mean-square fluctuation $F(\ell)$ of a time series within windows of ℓ points, and determines the correlation exponent α from the scaling function $F(\ell) \sim \ell^\alpha$. The exponent α is related to the autocorrelation function exponent γ by

$$\alpha = 1 - \gamma/2, \quad (12)$$

and autocorrelation function $C(t) \sim t^{-\gamma}$ where $0 < \gamma < 1$ [44,50]. When $\alpha > 0.5$, the time series has long-term correlations and exhibits persistent behavior, meaning that large values are more likely to be followed by large values and small values by small ones. The value $\alpha = 0.5$ indicates that the signal is uncorrelated (white noise).

We analyze the volatility series and the return interval series by using the DFA method. The results of S&P 500 index and 30 DJIA stocks for two regimes (split by $\ell^* = 390$ for volatilities and $\ell^* = 93$ for return intervals, which corresponds to 1 day in time scale) are shown in Fig. 8 [47]. We see that α values are distinctly different in the two regimes, and both of them are larger than 0.5, which indicates long-term correlations in the investigated time series but they are not the same for different time scales. For large scales ($\ell > \ell^*$), $\alpha = 0.98 \pm 0.04$ for the volatility (group mean \pm standard deviation) and $\alpha = 0.92 \pm 0.04$ for the return interval are almost the same, and the differences are within the error bars. These results are consistent with Refs. [33,43] for α of the volatilities, and with Ref. [43] for α of the return intervals. For short scales ($\ell < \ell^*$), we find $\alpha = 0.66 \pm 0.01$ for the volatility (consistent with Ref. [33]) and $\alpha = 0.64 \pm 0.02$ of the return intervals, and the differences are again in the range of the error bars. Here error bars refer to that of each dataset, not the standard deviation of α group for 31 datasets, and average error bars ≈ 0.06 . Similar crossover from short scales to large scales with similar values of α have been also observed for intertrade times by Ivanov *et al.* [51]. Such behavior suggests a common origin for the strong persistence of correlations in both volatility and return interval records, and in fact the clustering in return intervals is related to the known effect of volatility clustering [52–54].

VI. DISCUSSION AND CONCLUSION

The value of $\gamma \approx 0.4$ could be a result of $\gamma = 2 - 2\alpha$ from Eq. (12), where $\alpha \approx 0.8$ is the average of the two α regimes that we observe (see Fig. 8). It is possible for the value of γ

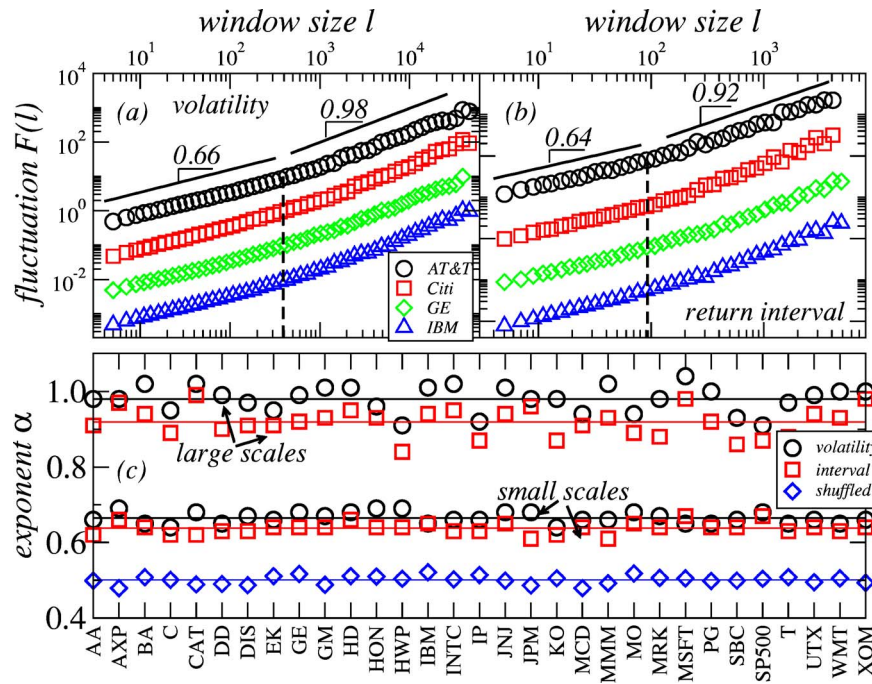


FIG. 8. (Color online) Root-mean-square fluctuation $F(\ell)$ for (a) volatility records and (b) return interval records ($q=2$) obtained by the DFA method. Four companies are shown, AT&T, Citi, GE, and IBM (each shifted by factor of 10). The range of window size is split by vertical dashed lines, $\ell^*=390$ for volatilities (sampled each minute) and $\ell^*=93$ for return intervals, both corresponding to a time window of 1 day. The two regimes have different correlation exponents, as indicated by the straight lines. (c) Correlation exponent α for 30 DJIA stocks and S&P 500 index (related stock names are shown in x axis). Volatility (circles) and return interval (squares) of large and smaller scales are shown. Note that most companies have a smaller exponent for intervals than for volatilities, but their differences still are in the range of the error bars. Shuffled records (diamonds) possess α values around 0.5 that indicate no correlation. Large scales ($\alpha=0.98\pm 0.04$ and $\alpha=0.92\pm 0.04$, group average \pm standard deviation for volatilities and intervals, respectively) and small scales ($\alpha=0.66\pm 0.01$ and $\alpha=0.64\pm 0.02$ correspondingly) show different correlations for different scales, since $\alpha > 0.5$.

to be different for small and large q values. The reason for these differences is that for small q the low volatilities are probed and therefore the time scales are controlled by $\alpha \approx 0.65$ (below the crossover), while for the large q the high volatilities are probed, which represent large time scales (above the crossover), controlled by $\alpha \approx 0.95$. We will undertake further analysis to test this possibility.

In summary, we studied scaling and memory effects in volatility return intervals for *intraday* data. We found that the distribution return function for the return intervals can be well-described by a single scaling function that depends only on the ratio of $\tau/\bar{\tau}$ for DJIA stocks and the S&P 500 index, for various time scales ranging from short term $\Delta t=1$ min to $\Delta t=30$ min. The scaling function, which results from the long-term correlations in the volatility records, differs from the Poisson distribution for uncorrelated data. We found that

the scaling function can be well-approximated by the stretched exponential form, $f(x) \sim e^{-ax^\gamma}$ with $\gamma=0.38\pm 0.05$ and $a=3.9\pm 0.5$. We showed strong memory effects by analyzing the conditional PDF $P_q(\tau|\tau_0)$ and mean return interval $\langle \tau|\tau_0 \rangle$. Furthermore, we studied the mean interval after a cluster of intervals, and found long-term memory for both clusters of short and long return intervals. We demonstrated by the DFA method that the volatility and return intervals have long-term correlations with similar correlation exponents.

ACKNOWLEDGMENTS

We thank L. Muchnik, J. Nagler, and I. Vodenska for helpful discussions and suggestions and the NSF and Merck Foundation for financial support.

- [1] *Econophysics: An Emerging Science*, edited by I. Kondor and J. Kertész (Kluwer, Dordrecht, 1999).
 [2] H. E. Stanley and V. Plerou, *Quant. Finance* **1**, 563 (2001).
 [3] R. Mantegna and H. E. Stanley, *Introduction to Econophysics: Correlations and Complexity in Finance* (Cambridge Univ. Press, Cambridge, England, 2000).

- [4] J.-P. Bouchaud and M. Potters, *Theory of Financial Risk and Derivative Pricing: From Statistical Physics to Risk Management* (Cambridge Univ. Press, Cambridge, England, 2003).
 [5] B. B. Mandelbrot, *J. Business* **36**, 394 (1963).
 [6] R. N. Mantegna and H. E. Stanley, *Nature (London)* **376**, 46 (1995).

- [7] H. Takayasu, H. Miura, T. Hirabayashi, and K. Hamada, *Physica A* **184**, 127 (1992); H. Takayasu, A. H. Sato, and M. Takayasu, *Phys. Rev. Lett.* **79**, 966 (1997); H. Takayasu and K. Okuyama, *Fractals* **6**, 67 (1998).
- [8] G. Caldarelli, M. Marsili, and Y.-C. Zhang, *Europhys. Lett.* **40**, 479 (1997); M. Marsili and Y.-C. Zhang, *Phys. Rev. Lett.* **80**, 2741 (1998).
- [9] D. Sornette, A. Johansen, and J.-P. Bouchaud, *J. Phys. I* **6**, 167 (1996); A. Arnoedo, J.-F. Muzy, and D. Sornette, *Eur. Phys. J. B* **2**, 277 (1998).
- [10] N. Vandewalle and M. Ausloos, *Int. J. Mod. Phys. C* **9**, 711 (1998); N. Vandewalle, P. Boveroux, A. Minguet, and M. Ausloos, *Physica A* **255**, 201 (1998).
- [11] S. Micciche, G. Bonanno, F. Lillo, and R. N. Mantegna, *Physica A* **314**, 756 (2002).
- [12] S. Picozzi and B. J. West, *Phys. Rev. E* **66**, 046118 (2002).
- [13] A. Krawiecki, J. A. Holyst, and D. Helbing, *Phys. Rev. Lett.* **89**, 158701 (2002).
- [14] D. D. Thomakos, T. Wang, and L. T. Wille, *Physica A* **312**, 505 (2002).
- [15] F. Lillo and R. N. Mantegna, *Phys. Rev. E* **62**, 6126 (2000).
- [16] K. Yamasaki, L. Muchnik, S. Havlin, A. Bunde, and H. E. Stanley, in *Proceedings of the Third Nikkei Econophysics Research Workshop and Symposium, The Fruits of Econophysics, Tokyo, November 2004*, edited by H. Takayasu (Springer-Verlag, Berlin, 2005).
- [17] N. F. Johnson, P. Jefferies, and P. M. Hui, *Financial Market Complexity* (Oxford Univ. Press, New York, 2003).
- [18] F. Black and M. Scholes, *J. Polit. Econ.* **81**, 637 (1973).
- [19] J. C. Cox and S. A. Ross, *J. Financ. Econ.* **3**, 145 (1976).
- [20] J. C. Cox, S. A. Ross, and M. Rubinstein, *J. Financ. Econ.* **7**, 229 (1979).
- [21] Z. Ding, C. W. J. Granger, and R. F. Engle, *J. Empirical Finance* **1**, 83 (1983).
- [22] R. A. Wood, T. H. McInish, and J. K. Ord, *J. Financ.* **40**, 723 (1985).
- [23] L. Harris, *J. Financ. Econ.* **16**, 99 (1986).
- [24] A. Admati and P. Pfleiderer, *Rev. Financ. Stud.* **1**, 3 (1988).
- [25] G. W. Schwert, *J. Financ.* **44**, 1115 (1989); K. Chan, K. C. Chan, and G. A. Karolyi, *Rev. Financ. Stud.* **4**, 657 (1991); T. Bollerslev, R. Y. Chou, and K. F. Kroner, *J. Econometr.* **52**, 5 (1992); A. R. Gallant, P. E. Rossi, and G. Tauchen, *Rev. Financ. Stud.* **5**, 199 (1992); B. Le Baron, *J. Business* **65**, 199 (1992).
- [26] M. M. Dacorogna, U. A. Muller, R. J. Nagler, R. B. Olsen, and O. V. Pictet, *J. Int. Money Finance* **12**, 413 (1993).
- [27] A. Pagan, *J. Empirical Finance* **3**, 15 (1996).
- [28] C. W. J. Granger and Z. Ding, *J. Econometr.* **73**, 61 (1996).
- [29] Y. Liu, P. Cizeau, M. Meyer, C.-K. Peng, and H. E. Stanley, *Physica A* **245**, 437 (1997).
- [30] R. Cont, Ph.D. thesis, Universite de Paris XI, 1998 (unpublished); see also e-print cond-mat/9705075.
- [31] P. Cizeau, Y. Liu, M. Meyer, C.-K. Peng, and H. E. Stanley, *Physica A* **245**, 441 (1997).
- [32] M. Pasquini and M. Serva, *Econ. Lett.* **65**, 275 (1999).
- [33] Y. Liu, P. Gopikrishnan, P. Cizeau, M. Meyer, C.-K. Peng, and H. E. Stanley, *Phys. Rev. E* **60**, 1390 (1999); V. Plerou, P. Gopikrishnan, X. Gabaix, L. A. Nunes Amaral, and H. E. Stanley, *Quant. Finance* **1**, 262 (2001); V. Plerou, P. Gopikrishnan, and H. E. Stanley, *Phys. Rev. E* **71**, 046131 (2005).
- [34] P. Gopikrishnan, M. Meyer, L. A. N. Amaral, and H. E. Stanley, *Eur. Phys. J. B* **3**, 139 (1998).
- [35] P. Gopikrishnan, V. Plerou, L. A. Nunes Amaral, M. Meyer, and H. E. Stanley, *Phys. Rev. E* **60**, 5305 (1999).
- [36] V. Plerou, P. Gopikrishnan, L. A. Nunes Amaral, M. Meyer, and H. E. Stanley, *Phys. Rev. E* **60**, 6519 (1999); V. Plerou, P. Gopikrishnan, L. A. Nunes Amaral, X. Gabaix, and H. E. Stanley, *ibid.* **62**, R3023 (2000); P. Gopikrishnan, V. Plerou, X. Gabaix, and H. E. Stanley, *ibid.* **62**, R4493 (2000);
- [37] X. Gabaix, P. Gopikrishnan, V. Plerou, and H. E. Stanley, *Nature (London)* **423**, 267 (2003).
- [38] X. Gabaix, P. Gopikrishnan, V. Plerou, and H. E. Stanley, *Quart. J. Econom.* 121 (to be published).
- [39] G. M. Viswanathan, U. L. Fulco, M. Lyra, and M. Serva, *Physica A* **329**, 273 (2003).
- [40] M. Serva, U. L. Fulco, I. M. Gleria, M. Lyra, F. Petroni, and G. M. Viswanathan, *Physica A* (to be published).
- [41] F. Lillo and R. N. Mantegna, *Phys. Rev. E* **68**, 016119 (2003).
- [42] F. Omori, *J. Coll. Sci., Imp. Univ. Tokyo* **7**, 111 (1894).
- [43] K. Yamasaki, L. Muchnik, S. Havlin, A. Bunde, and H. E. Stanley, *Proc. Natl. Acad. Sci. U.S.A.* **102**, 9424 (2005).
- [44] A. Bunde, J. F. Eichner, J. W. Kantelhardt, and S. Havlin, *Phys. Rev. Lett.* **94**, 048701 (2005).
- [45] *Fractals in Science*, edited by A. Bunde and S. Havlin (Springer, Heidelberg, 1994).
- [46] M. Constantin and S. Das Sarma, *Phys. Rev. E* **72**, 051106 (2005).
- [47] C.-K. Peng, S. V. Buldyrev, S. Havlin, M. Simons, H. E. Stanley, and A. L. Goldberger, *Phys. Rev. E* **49**, 1685 (1994); C.-K. Peng, S. Havlin, H. E. Stanley, and A. L. Goldberger, *Chaos* **5**, 82 (1995).
- [48] K. Hu, P. Ch. Ivanov, Z. Chen, P. Carpena, and H. E. Stanley, *Phys. Rev. E* **64**, 011114 (2001); Z. Chen, P. Ch. Ivanov, K. Hu, and H. E. Stanley, *ibid.* **65**, 041107 (2002); L. Xu, P. Ch. Ivanov, K. Hu, Z. Chen, A. Carbone, and H. E. Stanley, *ibid.* **71**, 051101 (2005); Z. Chen, K. Hu, P. Carpena, P. Bernaola-Galvan, H. E. Stanley, and P. Ch. Ivanov, *ibid.* **71**, 011104 (2005); J. W. Kantelhardt, S. Zschiegner, E. Koscielny-Bunde, S. Havlin, A. Bunde, and H. E. Stanley, *Physica A* **316**, 87 (2002).
- [49] A. Bunde, S. Havlin, J. W. Kantelhardt, T. Penzel, J.-H. Peter, and K. Voigt, *Phys. Rev. Lett.* **85**, 3736 (2000).
- [50] E. Koscielny-Bunde, A. Bunde, S. Havlin, H. E. Roman, Y. Goldreich, and H.-J. Schellnhuber, *Phys. Rev. Lett.* **81**, 729 (1998).
- [51] P. Ch. Ivanov, A. Yuen, B. Podobnik, and Y. Lee, *Phys. Rev. E* **69**, 056107 (2004).
- [52] T. Lux and M. Marchesi, *Int. J. Theor. Appl. Finance* **3**, 675 (2000).
- [53] I. Giardina and J. P. Bouchaud, *Physica A* **299**, 28 (2001).
- [54] T. Lux and M. Ausloos, in *The Science of Disasters: Climate Disruptions, Heart Attacks, and Market Crashes*, edited by A. Bunde, J. Kropp, and H. J. Schellnhuber (Springer, Berlin, 2002), pp. 373–409.